Manifestations of Symmetry Breaking in Self-consistent Field Electronic Structure Calculations

Barry D. Dunietz and Martin Head-Gordon*

Department of Chemistry, University of California at Berkeley, and Chemical Sciences Division, Lawrence Berkeley National Laboratory, Berkeley, California 94720

Received: November 21, 2002

Studies of symmetry-breaking are reported for self-consistent field wave functions applied to three homonuclear diatomics: F_2^+, O_2^+, and Cr_2. The results complement and extend existing reports on symmetry-breaking in three main ways. Two of these aspects concern manifestations of symmetry-breaking. First, calculations are reported that show energies at long interatomic separations which are lower than the sum of the atomic limits. This artifactual behavior, observed both with Hartree−Fock and Kohn−Sham density functional theory, appears to be largely associated with insufficiently flexible atomic orbital basis sets. Second, potential curves with spurious maxima and minima are found, associated with changes in spin-coupling. The third and final aspect, concerns the origin of symmetry-breaking. It is argued that the simplest way to understand symmetry breaking is as a consequence of the incorrect asymptotic behavior of limited wave functions at long interatomic distances.

Introduction

The calculation of potential energy surfaces (PES's) is of central importance in chemistry. They are used to provide insight into chemical reactions by following the geometries of the system along a reaction coordinate.

It is well-known that *exact* solutions of the Schrödinger equation *must* conform to the symmetry of the molecule, since symmetry operators commute with the Hamiltonian. For approximate solutions, however, this is not necessarily true. A trial wave function with limited flexibility may achieve a lower energy by breaking symmetry than is possible with the additional constraint of respecting it. The occurrence of symmetry broken solutions is troublesome. The "dilemma",[1] often described as "symmetry-breaking" (SB), is which wave function should be regarded as the "correct" solution? Is it a higher energy answer with correct symmetry or the lower energy solution with broken symmetry?

While symmetry-breaking, by definition, only manifests itself in systems with point group symmetry, it is a signature of more general problems associated with restricted wave functions. For example, while the homonuclear diatomics O_2^+ [2,3] and F_2^+ [3−5] are well-known for symmetry-breaking (and indeed are part of this study), a recent survey[6] of the performance of electronic structure methods for radicals found that their isoelectronic species NO and OF were particularly problematic even for high-level methods.

Explicit avoidance of symmetry-breaking by simply imposing the appropriate symmetry constraints on the calculated wave function is not satisfactory. It becomes clear from experimentation that this produces low quality wave functions, which for example do not separate correctly into atomic fragments as bonds are being broken. Furthermore, discontinuities in the PES are often unavoidable in this approach, since the constrained solution is often not a true minimum, and it can no longer be defined if the molecular framework distorts to a lower symmetry.

Artifactual SB is to be regarded separately from "legitimate" SB originating from Jahn−Teller[7] effects as has been defined by Borden and Davidson.[8] Needless to say, it is not always easy to distinguish them in practice. SB is often associated with systems having more than a single dominant valence bond structure (or any localized orbital structure). An approximate wave function such as a single determinant cannot always achieve this mixing with symmetric orbitals. In such cases, it may obtain a lower energy by breaking symmetry and localizing to a single valence structure. This occurs, for example on parts of the NO_2 potential surface calculated by restricted open shell HF (ROHF).[9]

In the picture of McLean et al.,[10] SB in an approximate wave function arises from the competition between the energetic stabilization that comes from *orbital size effects* and *resonance effects*. SB first occurs at the point along the relevant coordinate of the potential at which orbital size effects become dominant over resonance effects. At the SB point, it becomes energetically favorable for the wave function to describe more accurately a specific local structure (and thus break symmetry) rather than allow full resonance among the energetically low-lying local structures.

Various approaches have been designed to describe the resonance between the localized structures. It is possible to systematically include the configurations necessary to describe the localized structures starting from symmetric orbitals.[10] However, many configurations are often required to overcome the SB.[11−13]

Alternatively a very compact description can be obtained, following Jackels and Davidson,[9] by performing a small nonorthogonal CI in the basis of the localized structures. This method has been used in subsequent studies on O_4^+ [12] and formyloxyl radical.[14] The same basic idea is also exploited in the generalized resonating valence bond approach,[15,16] the breathing orbitals valence bond method,[17] and the generalized multistructure wave function.[18] In all these methods, each structure is essentially assigned a separate set of orbitals.

The performance of coupled cluster (CC) methods for removing SB effects has been tested in numerous studies.[19]

10.1021/jp0224665 CCC: $25.00
Published on Web 10/08/2003

Generally speaking, CC methods which do not vary the orbitals are still affected by SB in these reference orbitals, although to a substantially reduced degree (particularly as the level of retained excitations increases). Varying the reference orbitals as in Brueckner CC (BCC) methods can eliminate SB in principle (if sufficiently high excitations are retained). In practice Brueckner doubles (BD) suffice to cure symmetry breaking in some applications[20,21] but not in others.[22,23]

Modern gradient-corrected density functional theory (DFT) methods have also been tested for their treatment of SB problems. Generally they are more resistant to SB than Hartree−Fock methods—in the sense of exhibiting SB further toward dissociation such that equilibrium molecular properties are less affected.[3,6,24,25] However, this resistance to SB in DFT is actually associated with some severe problems in dissociation, such as qualitatively incorrect curves for systems as simple as H_2^+ and He_2^+.[26−28] Thus, DFT is certainly the self-consistent field method of choice, but (at least with present-day functionals) it is not always a panacea for SB problems.

The point at which SB occurs can be characterized by stability theory.[11] Paldus and Cizek[29−33] were the first to formulate mathematical conditions for the stability of a symmetry-adapted wave function. Connections between orbital instability points and anomalous force constants have been further investigated[11,34] and a relation between negative Hessian values and orbital instabilities has been suggested.

Crawford et al.[19] have shown that near zero values in the Hessian are associated with anomalous predictions of vibration modes. However, it remains still unclear what is "near zero". Cases with rather small Hessian values have been identified where symmetry breaking does *not* occur while other cases with larger Hessian values have suffered from instabilities. Concerning O_2^+ and F_2^+, Cohen and Sherrill[3] recently concluded that "directly attributing anomalous property predictions to negative or small MO Hessian eigenvalues or to pseudo-Jahn−Teller interactions does not appear to explain all of our results". Thus, "the connection between SB and spurious molecular property predictions remains unclear for these cases."

In this paper, we revisit the problem of SB in self-consistent field wave functions for three homonuclear diatomic molecules: F_2^+, O_2^+, and Cr_2. The main purposes of this paper are as follows. First, while F_2^+ and O_2^+ are already well-studied problems, the main focus of previous reports has been poorly predicted properties at equilibrium due to SB effects, and the search for methods sophisticated enough to overcome the failures of simpler theories. Here we focus on understanding the origin of SB in terms of the dissociation behavior of the single determinant wave function. Whenever symmetry restrictions prevent the wave function from obtaining the lowest energy solution at long separations, SB must occur, and can be understood from this physical point of view (although the exact point of SB cannot, of course, be predicted except by stability analysis).

The second purpose of this paper is to report and explain two additional forms of SB. One concerns obtaining energies at long bond lengths that are *below* the sum of separate atomic energies under conditions that appear to be directly associated with the use of insufficiently flexible basis sets. Another concerns obtaining spurious stationary points on potential energy surfaces due to changes in spin-coupling in unrestricted single determinant wave functions. Just as the restricted form of the SCF (or any other kind of) wave function leads to SB, false maxima (or minima) on the potential curve may also arise due to strong variations in the character of the calculated wave function.

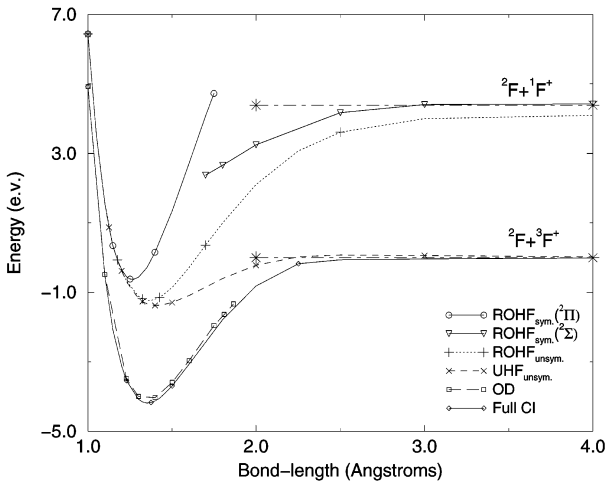

Figure 1. F_2^+ HFs., OD, and FCI wave functions at the minimal basis set. The lowest energy separated atoms state was used as the zero energy state. *Note, in all figures not all the calculated points have been marked by an appropriate symbol.*

Results and Discussion

Our calculations on F_2^+, O_2^+, and Cr_2 are presented and discussed in the following three subsections. For the first two systems, we performed calculations in the minimal STO-3G basis because of the ease of analysis, and the ability to readily obtain exact full configuration interaction (FCI) results. We then use the 6-31G* basis for subsequent calculations. For Cr_2, we present calculations using the recently defined 6-31G* basis,[35] and also the much larger Wachters[36] + f basis, as used in previous studies of this molecule.[37] SCF calculations were performed with the Q-Chem program,[38] using geometric direct minimization[39,40] to obtain convergence. FCI calculations were performed using PSI.[41]

F_2^+ Cation. There have been numerous previous studies of F_2^+, a system notoriously known for SB. For example, Murphy et al.[4] used SCF and many body perturbation theories, Watts and Bartlett[5] employed CC methods, and Cohen and Sherrill[3] evaluated DFT.

Figure 1 presents the different STO-3G potential surfaces available at HF level for the F_2^+ molecule. Also included (in the figure) are the curves for full CI (FCI) and the optimized orbitals coupled cluster doubles (OD) wave function[42] (CCD with variationally determined Brueckner orbitals). We consider the origin of the various SCF curves in the following paragraphs, starting from the most constrained solutions (the 2 symmetric ROHF solutions), then releasing the ROHF symmetry constraint, and finally also releasing the spin symmetry constraint. HF curves are also shown in the 6-31G* basis set in Figure 2.

At the equilibrium geometry the ground state has $^2\Pi_g$ symmetry. This suggests the wave function corresponds primarily to the following configuration:

$$\Psi_{^2\Pi_g} = ...(\sigma_g)^2(\pi_u)^4(\pi_g^*)^3 \qquad (1)$$

where we have considered only molecular orbitals (MO's) originating from the 2p atomic orbitals (AO's). The bond order (BO) of this configuration is 3/2, corresponding to a single bond and a three-electron bond. The three-electron bond[43,44] consists of a singly occupied antibonding π^* orbital and the correspond-

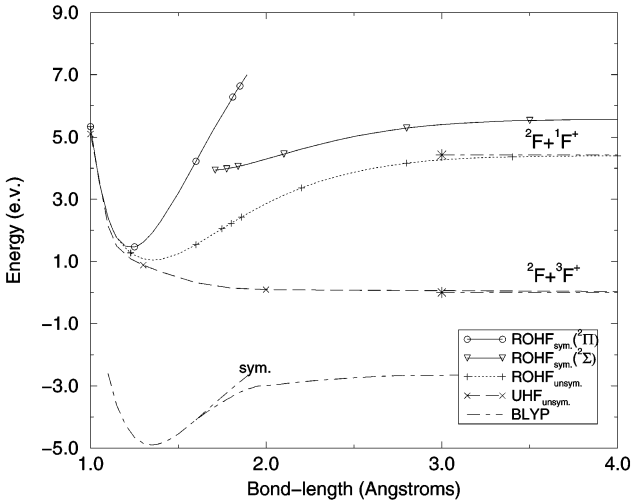

Figure 2. F_2^+ HFs. and BLYP wave functions at 6-31G* basis set. The lowest energy separated atoms state was used as the zero energy state (with the relevant method).

ing bonding π orbital is doubly occupied. The Lewis dot structure of this molecular configuration can be described as

Only well-correlated wave functions can describe this state symmetrically with all five electrons, which participate in the bonding, delocalized between the two atom centers.

The ROHF curve describing this wave function is shown in the figure, but cannot be followed far beyond equilibrium. This wave function cannot dissociate to the correct ground-state atomic products (triplet F^+ and doublet F), or even any separable atomic products because of its restricted form. However, there is a higher state, of $^2\Sigma_g^+$ symmetry, which can dissociate properly within the constraints of a symmetric ROHF solution. In this state, relative to the $^2\Pi$ ground state, a σ_g electron has been promoted to the π_g^* orbital. Thus:

$$\Psi_{^2\Sigma_g^+} = ...(\sigma_g)^1(\pi_g)^4(\pi_u^*)^4 \qquad (2)$$

The BO of this $\Psi_{^2\Sigma^+_g}$ state is only $^1/_2$, and, as a quasi-one-electron problem, dissociation to singlet F^+ and doublet F can be described by the ROHF wave function. A Lewis dot structure describing this state is

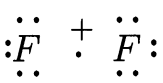

Let us now turn to the origin of spatial symmetry breaking for ROHF. First, we would like to concentrate on the ground-state potential curve. (This is the ground state at the vicinity of the equilibrium distance.) However, this $^2\Pi_g$ state with the symmetrical constraint is high in energy at already small bond stretches. The expected atomic limit of this stretch, on the other hand, lies much lower in energy. The consequence of this is clear. There has to exist a solution which reaches, as the bond is stretched to large numbers, an atomic limit. The atomic limit is achieved by breaking the molecular symmetry of the wave function, where the charge is localized on one of the atoms.

Knowing that we cannot correctly reach the ground-state atomic products with the ROHF form, the effect of spatial symmetry breaking would be expected to yield the energy separated atoms solution, $^2F + {}^1F^+$. This asymptote would be connected eventually to the $^2\Pi_g$ solution which is most stable via ROHF at sufficiently short bond lengths. Inspection of the SB ROHF curve in Figure 1 shows that this is qualitatively true. However, there is a surprise: at long separations, an energy slightly lower than the sum of the noninteracting atoms is obtained. Inspection of the charges on the atomic products shows that there is not a complete separation of the charge, but one atom has charge $+0.85$ and the other $+0.15$. A similar tendency is well documented for radical ions with DFT calculations.[26−28] However, it is expected that HF calculations will demonstrate the "obvious" degeneracy in energy of the two localized structures and any linear combinations of them[26] at large separations.

Why is the nonseparable solution found, although the correct limit can in principle be achieved? Evidently it is energetically advantageous for the two systems to exchange electrons, such that the solution is a statistical mixture of F^+/F and F/F^+, in obvious contradiction to physical intuition, and exact theory,[45] which says there should be no energy gain. However, consider a solution in which one F was exactly neutral (a doublet) and the other cationic (a singlet). Charge exchange between the two units can occur if the ionization potential (IP) of the neutral atom is less or equal than the negative of the electron affinity (EA) of the cationic atom (with the orbitals fixed).

The charge-transfer resulting in the energy lowering can be symbolized by the following Lewis dot structure of the relevant atoms:

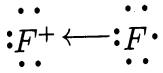

The actual energy lowering is 0.009 au at the minimal basis set. In the minimal STO-3G basis, the IP and EA are equal because each charge state has identical orbitals. Note, however, that the IP and EA provide only a partial description of the condition for the charge-transfer process to occur. $\partial E/\partial N$, the derivative of the energy with respect to change of number of electrons in the subsystem, is constant only in exact theory. The IP and EA provide this information only at the integral values of N, and since ROHF is an approximate theory, the curvature of the derivative yields energy gain at the minimal basis set. In the larger 6-31G* basis, the comparison of the IP and EA indicates that this charge transfer is unlikely to occur (even with the curvature considered). The values of EA and IP were calculated to be -0.6 and 0.8 au, respectively, indicating that charge transfer will not occur.

Since the two structures considered in the charge-transfer process, F^+/F and F/F^+, use just one set of orbitals, the IP and EA are slightly different than the usual definition of these quantities. Here, we refer to the EA/IP of one atom with the optimized orbitals of the other atom. In our case, the EA of the cation is calculated using the orbitals of the neutral atom, while the IP of the atom is calculated with the optimized orbitals of the cation. This is well described in the following equations:

$$\mathrm{EA}(F^+) = E(F/F^+) - E(F^+/F^+) \qquad (3)$$

$$\mathrm{IP}(F) = E(F^+/F) - E(F/F) \qquad (4)$$

Clearly, only the total number of electrons N ($N = N_F + N_{F^+}$) is conserved, while the numbers of the electrons in the subsystems (N_F, N_{F^+}) are not. However, a single Fock operator describes the electron−electron interactions, and furthermore only a single set of orbitals describes the system. This is clearly different from the proper treatment of the statistical mixture

TABLE 1: Charge Separation and Interatomic Fock Elements Correpsonding to Restricted HF Wave Function of F_2^+

separation (Å)	energy (au)	maximum $F(2p_1 - 2p_2)$	charge
	Minimal Basis Set		
1.3	−195.5508	0.673	0.407
1.5	−195.5414	0.479	0.489
1.6	−195.5206	0.401	0.465
2.0	−195.4325	0.194	0.318
4.0	−195.3596	−0.0306	0.155
6.0	−195.3587	−0.0216	0.148
7.0	−195.3583	0.0176	0.146
17.5	−195.3580	0.00449	0.139
20.5	−195.3579	0.00306	0.138
22.5	−195.3579	−0.00259	0.138
	6-31G* Basis Set		
1.75	−198.0816	0.139	0.382
1.80	−198.0753	0.123	0.358
2.0	−198.0520	0.0810	0.272
2.4	−198.0200	0.0442	0.145
3.1	−197.9990	0.0157	0.0275
3.7	−197.9959	0.003 09	0.001 45
4.0	−197.9955	0.000921	0.000164
4.5	−197.9951	0.0000554	0.000001
5.0	−197.9949	0.0000070	0.000000

where each pure component interacts according to its own Fock operator, with its own independently optimized wave function. In other words, since the Fock operators of the different atomic states are not orthogonal the overall Fock operator (when charge is allowed to be transferred) represents a linear combination of the different states. Therefore, an artificial interaction is induced between the two components of the statistical mixture. This means that the energy, as a function of the amount of charge exchanged, is not invariant, but instead can be lowered.

The consequence of the charge-transfer allowed (by inspecting the IP and EA values) at the minimal basis set is the energy lowering obtained at the asymptotic region of the curve. Table 1 provides an additional description of this effect. By listing the charges of one of the atoms at different separations, it is demonstrated that complete charge separation is obtained only with the larger basis set. On the other hand, the asymptotic limit for the minimal basis set is a mixture of the pure charge states. This information is also established by observing the overall Fock matrix. In the table, the largest Fock element between 2p orbitals from the different atoms is listed as a function of the atom separation distance. These elements vanish in the case were the atoms do not interact (larger basis set and distances). It is demonstrated that these elements reach a nonvanishing asymptotic value at large separations with the minimal basis set where energy lowering is obtained.

The atomic separation limit for the restricted-spin calculation is the combination of the cation singlet ($F^+(^1P_2)$) and the doublet F atom ($F(^2P_{3/2})$). However, the ground state of the separated atoms is defined by the triplet coupling of the cation ($F^+(^3P_2)$). The energy of this state lies much lower than the atomic limit of the spin-restricted curve. The consequence of this is also clear. This correct limit can be reached only by also releasing the spin restriction.

The unrestricted HF (UHF) curve is shown to reach at "infinite" separation the energetically lowest dissociation limit. This is achieved by breaking the spin symmetry (in addition to the breaking of the molecular symmetry). The spin-symmetry breaking point of the unsymmetric (US) curve occurs before the equilibrium distance but slightly after the molecular SB of the spin-restricted curve. Namely, the spatial symmetry broken solution of a radical system may still obey the spin symmetry. This is despite the implicit asymmetry of spin occupation in radical systems. Beyond the spin-SB point, both of the US lines continue to reach their appropriate atomic separation limits. Therefore, the spatial symmetry breaking is not related directly to the spin symmetry even with radical systems. Instead it is related to the asymptotic limit.

The resulting US−ROHF curve is shown to fix the problematic behavior of the symmetric curve by widening the potential well and thus extending the equilibrium distance. This, by comparing to the "exact" result calculated by the FCI, generates an improvement in the quality of the results. The US−ROHF predicts a 1.375 Å equilibrium distance. This is a small improvement over the symmetric curve (1.27 Å), when compared to the "exact" result defined by the FCI (1.35 Å). Also note that the form of the potential-well of both the US−ROHF and FCI is similar. However, this similarity is coincidental. As shown in Figure 1, the energy difference between the two atomic limits (spin restricted and spin unrestricted cases) is similar to the correlation energy at the equilibrium distance region. Thus, the more accurate equilibrium geometry (cf. FCI) obtained by SB ROHF vs SB UHF is a result of the incorrect asymptote of the former! This point is even clearer in Figure 2 with the 6-31G* basis, where SB UHF, dissociating to the correct atomic products, is unbound, while SB ROHF is bound only because it dissociates to excited atomic products.

This highlights the point that only correlated methods are able to describe both the correct asymptotic atomic limit and the bound equilibrium region in a balanced way. As discussed above, methodologies based on multiconfigurational approaches have been able to achieve this goal, as have coupled-cluster (CC) methods. For example, in Figure 1, the OD curve is shown to reproduce the FCI result up to a distance of 2 Å.

Modern density functional theory (DFT) offers another possible alternative to treat SB effects. To some extent, DFT methods achieve the goal of deferring SB occurrence away from the molecular region.[25,26] However, the limitations of the BLYP functional are on display even for this problem. In Figure 2, we have provided the BLYP bond energy curves calculated with the 6-31G* basis set. The symmetry breaking point is shown to occur further away from the equilibrium region than the corresponding point at the HF level (around 1.6 Å for DFT). However, while the behavior around equilibrium is quite good, as already noted,[26] at longer bond-lengths, the behavior is pathological. An asymptote is achieved which is below the sum of the atomic limits, reflecting limitations of this exchange functional. An unphysical low lying asymptote is observed for both symmetric (not shown) and unsymmetric curves emphasizing the failure of this functional in the dissociation limit; a failure which is believed to be associated with spurious self-interaction effects.[26]

O_2^+ Cation. Now, we are ready to turn to the second molecule considered in this work, the O_2^+ molecule. The O_2^+ is another well-known case exhibiting SB. Chandrasekher et al.[2] have shown that CCSD performs better than CCSD(T) when attempting to recover from a SB solution for O_2, O_2^+, and O_2^-. This highlights, again, the need to vary the orbitals of the SB solution.

Figure 3 presents the different HF PESs for this system. Similar observations underlying the SB occurrence can be done for this system as done above with F_2^+. The only significant qualitative difference is that the order at which the SB are occurring is reversed when compared to F_2^+. Namely, for O_2^+ the break of the spin-symmetry occurs before the molecular SB point of the ROHF function.

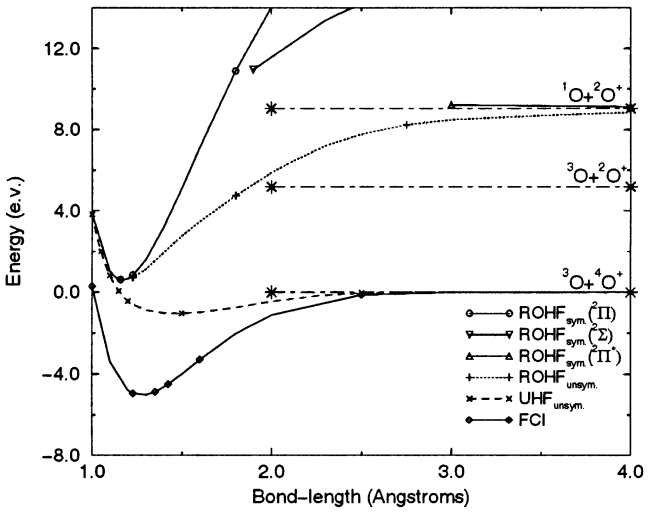

Figure 3. O_2^+ HFs. and FCI wave functions at the minimal basis set. The lowest energy separated atoms state was used as the zero energy state.

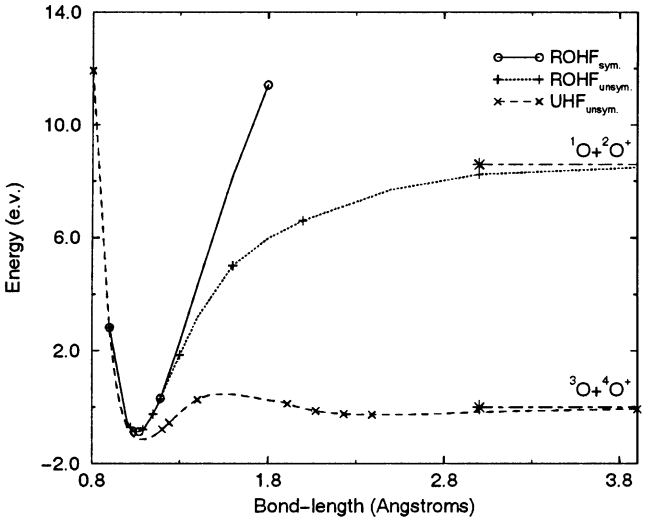

Figure 4. O_2^+ HFs. wave functions at 6-31G* basis set. The lowest energy separated atoms state was used as the zero energy state.

The O_2^+ molecule has two electrons less than F_2^+ and thus a higher bond order. The ground state at the equilibrium geometry is also a $^2\Pi_g$ state. It is given by

$$\Psi_{^2\Pi_g} = ..(\sigma_g)^2(\pi_u)^4(\pi_g^*) \quad (5)$$

The BO is $^5/_2$. At a bond length of 2 Å a $^2\Sigma_g^+$ state becomes lower in energy. This is achieved by promoting an electron from the σ_g orbital to a π_g^* orbital (BO is $^3/_2$):

$$\Psi_{^2\Sigma_g^+} = ..(\sigma_g)^1(\pi_u)^4(\pi_g^*)^2 \quad (6)$$

Finally, an additional state, with a BO of $^1/_2$, can be observed. This is obtained by promoting the second σ electron to the π^* shell:

$$\Psi_{^2\Pi_g^*} = ..(\sigma_g)^0(\pi_u)^4(\pi_g^*)^3 \quad (7)$$

Note that this state has a 3-electron bond resulting in $^1/_2$ BO. An appropriate Lewis dot structure description for this state is

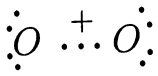

This state can be shown to reach the correct atomic separation limit for the ROHF function (in contrast to the other two considered above). At the minimal basis set, bonds defined by a single pair of bonding and antibonding orbitals, can be described symmetrically also at infinite separations. However, the binding states, which are much more stable at the equilibrium geometries, are shown to have high energies, when stretched symmetrically, at large separations. This underlies the occurrence of SB.

As discussed above, the atomic separation limit for the restricted-spin calculation has to be a combination of a singlet atom center and a doublet atom center. These are the doublet cation ($^2O^+$) and the singlet atom (^1O). The symmetric potential curve of the ground state rises steeply above the sum of the energies of these atoms. By breaking the molecular symmetry, the ROHF is able to lower the energy and reach (close to) the atomic separation limit. The US−ROHF curve is shown to widen the potential well. The shape of the US−ROHF potential well is similar to that of the FCI. However, the SB point occurs (slightly) after the equilibrium point. Thus, the equilibrium distance is not extended toward the FCI result by the SB at the ROHF level.

The energy level of the US−ROHF curve is shown to reach just below the sum of the energies of the doublet and singlet atoms at large separations. The US−ROHF converges to a state which lies 0.009 a.u. below the direct sum of the atoms energies, with charges of 0.85 and 0.15 a.u. on the atom centers. This is very similar to what has been observed with the F_2^+ molecule. (This is less evident in Figure 3, because the coordinate scaling is different.)

The ground state of the separated atoms involves the triplet spin coupling of the oxygen atom (^3O). The energetic state of this state lies much lower than the atomic limit of the spin-restricted case. Furthermore, the equilibrium energy of the symmetrical ROHF ground-state lies *above* the energies of the ground states of the atoms. The consequence is again the unavoidable SB exhibited by the US−UHF curve. The ground state dissociation limit can be reached only by releasing the spin restriction. The UHF curve is shown to reach at "infinite" separation the energetically lowest atomic states. This SB point *has* to occur before the equilibrium point. The resulting curve for the US−UHF is also very flat, which demonstrates again the importance of the treatment of correlation in order to achieve a reasonable description of the system.

Next, we will consider the HF curves for the O_2^+ molecule with the 6-31G* basis set. Figure 4 presents these curves. SB is again anticipated by observing the symmetric curve in relation to the energies of the correct separate atoms limits. The US−UHF for this system, however, demonstrates an additional interesting point: it exhibits a strong maximum. This occurs in the spin recoupling region, where the system is changing to a state of high spin coupling within the separating atoms ($^4O^+$,^3O) from a state which was essentially doublet coupling of all valence electrons. False maxima of US−UHF have been observed in the other systems but were less noticeable. Figures 5 and 6 present the low spin UHF and the high spin (sextet) UHF curves for the O_2^+ molecule at the 6-31G* and minimal basis sets, respectively.

These curves explain the absence of a strong maximum with the minimal basis set in contrast to the strong maximum observed at the larger basis set. The effect of the larger basis set has pushed the low spin energy curve to the left, which is reducing the equilibrium distance. Thus, the crossing of the low

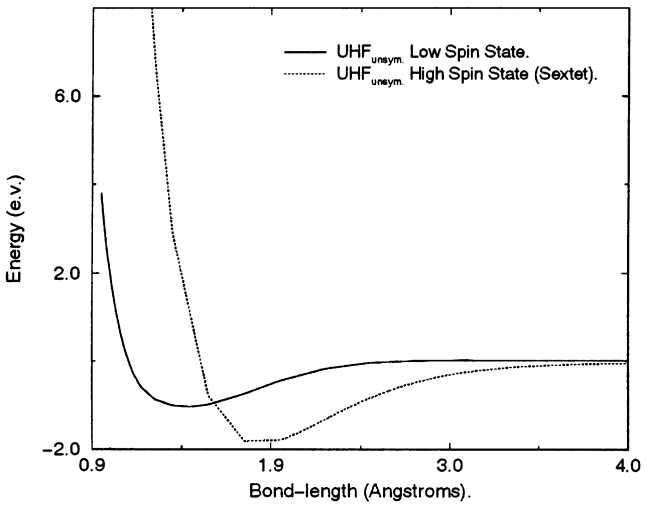

Figure 5. O_2^+: low and high spin-coupling of US−UHF wave function at the minimal basis set. The lowest energy separated atoms state was used as the zero energy state.

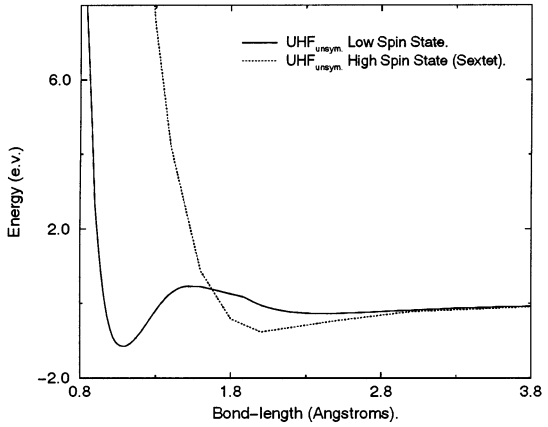

Figure 6. O_2^+: low and high spin coupling of the US−UHF wave functions at the 6-31G* basis set. The crossing of the states occurs further away from the minimum point of the doublet spin-coupled potential. The lowest energy separated atoms state was used as the zero energy state.

spin coupling and the high spin coupling curves occurs further away (to the right) from the equilibrium point. Hence, the system transfers to the high spin coupling at a relatively high energy on the low spin energy curve. This is causing the curve to drop when reaching stretches that are in a region dominated by the high spin coupling. At the minimal basis set, on the other hand, this crossing occurs much closer to the equilibrium distance of the doublet. Hence, at the spin recoupling region, the potential surface is still low enough to be able to transfer smoothly to the high spin-coupling region.

Cr_2 Molecule. The tendency of DFT calculations to defer SB has been noted before.[25] For systems with three electron bonds, DFT was shown to overestimate the strength of the bonding.[27] These two observations are related since the description of the localized structure is not well treated by current DFT methodologies (although progress in that regard has been reported[46]). Another consequence of this character of DFT calculations is the wrong asymptote obtained for radical systems,[26] where a solution with energy lower than the expected energies of the corresponding subsystems is obtained at large separations. In this section we provide results demonstrating that this is not limited to radical ions. The Cr_2 molecule provides another manifestation of this artifact arising in SCF calculations due to limitations imposed in the calculation.

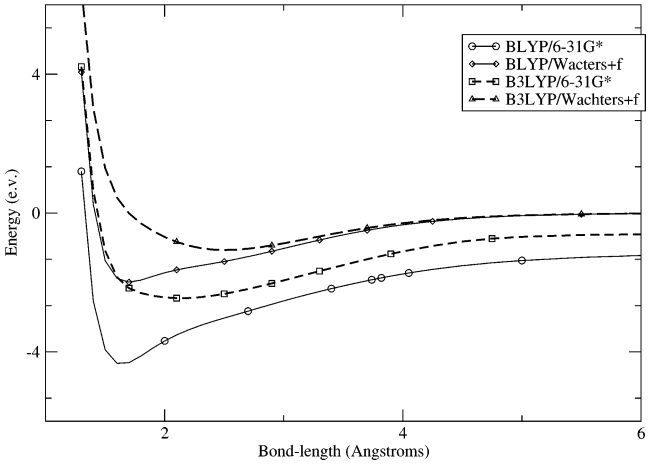

Figure 7. Cr_2: binding energy (eV) of the Cr_2 molecule with respect to the atoms separation calculated by DFT (BLYP and B3LYP) method with 6-31G* basis set and Wachters+f function special basis set. Note, the stabilization energy obtained by the DFT functionals at the asymptotic region, which is eliminated at the improved basis set.

The Cr_2 dimer has been extensively investigated due to its challenging character. The outer electronic shell of a Cr atom is $3d^54s^1$, containing six unpaired electrons. The 12 electrons in the dimer are all coupled to create a singlet state in the molecule. The change from 12 unpaired electrons in the separated atoms to all singlet coupled in the molecule underlies the complexity of the calculation. In addition the different interactions of the valence shells (3d−3d and 4s−4s) add to the complexity, and it may still be an open question whether the potential energy curve involves two minima or one minimum and one shelf. The unusual bonding in Cr_2 is well demonstrated in its very short bond length (1.67 Å) along with its small bond energy.

Different methodologies have been applied to this problem in efforts to obtain a faithful description. These studies include coupled cluster calculations,[37,47] multiconfigurational based approaches involving CASPT2,[48,49] generalized valence-bond studies,[50] and recent large MR−CI[51] and different DFT studies.[37,52] In this study, however, we focus on the demonstration of SB effects involved with DFT calculations of the Cr_2 dimer.

In Figure 7, we plot the bond energy as a function of the separation of the two atoms. This energy is simply the difference between the energy of the molecular calculation and twice the energy of the isolated atom (at high spin state). For Cr_2, we note that the bond energy remains negative (i.e., favoring the bonding) at large separations for the functionals (BLYP and B3LYP) tested with the 6-31G* basis set. The binding energy at 7.0 Å is −1.2 and −0.6 eV for BLYP and B3LYP, respectively. This is qualitatively similar to the ROHF wave function behavior for the radicals discussed in detail above at the minimal basis set. This SB can be eliminated by improving the basis set used in the calculation. In the figure it is demonstrated that with an improved basis set,[37] the Wachters basis set augmented with f functions, both BLYP and B3LYP are able to predict the correct asymptotic limit. The curves of the larger basis set are shifted toward smaller binding energy when compared to the offending curves at the 6-31G* basis set. This emphasizes the need to perform DFT calculations with large basis sets. Since the functionals are developed at the basis set limit they may perform poorly in small basis sets.

The origin of the 6-31G* symmetry breaking at the asymptotic region in this case is different than with the radical

TABLE 2: Energies of Different Spin State Mixtures of a Single Cr Atom at the Different Functionals and Basis Sets Considered

lowest spin coupling	energy (au)
BLYP/6-31G*	
7	−1044.2817
5	−1044.2967
BLYP/Wachters	
7	−1044.4420
5	−1044.4123
B3LYP/6-31G*	
7	−1044.2787
5	−1044.2967
B3LYP/Wachters	
7	−1044.4246
5	−1044.3956

TABLE 3: Fock Matrix Elements Involving Orbitals of the Two Atoms at 7.0 Å Separation Calculated by BLYP/6-31G*

orbitals	matrix value (au)
4s−5s	0.0000061
4s−5p	0.0000324
4p−5s	0.0000162
4p−5p	0.0000812
5s−5s	0.0000986
5s−5p	0.0003364
5p−5p	0.0010183

discussed above. Cr_2 has a complicated spin space, where at the asymptotic region 6 spins of each atom need to be parallel. These parallel spins on the two atoms are then low-spin coupled to obtain the "molecular" singlet spin coupling. However, the possibility to have a spin broken solution allows the spins of electrons of opposite atoms to interact such that the solution is a mixture of spin states where the spins are either aligned or at opposite directions. This mixture which describes the atom at large separations is absent when performing a high spin single atom calculation. Table 2 lists the atomic energies of the Cr atom at the different basis sets and functionals. It is demonstrated that in fact the high spin state is not the lowest energetic state at the smaller basis set for both functionals. The spurious stabilization energy at large separations is reduced from 1.2 to 0.33 eV for BLYP and from 0.6 to 0.36 eV for the B3LYP functional when the lowest atomic energies are considered. The remaining stabilization energy originates from the additional spin interaction which is possible due to the overall molecular singlet spin coupling where the spin broken solution involves spin recouplings absent in the single atomic calculations.

However, the mechanism by which a spurious energy gain is obtained is also similar to the mechanism by which a low asymptotic limit is reached by the F_2^+ radical system as described above. In regard to the radicals, we have noted that a spurious energy gain can be obtained by a mechanism of charge transfer, where different charge states interact. Here, the role of charge is replaced by spin flips such that the gain in energy stabilization is obtained by interaction of different spin coupling states. The consequence of this interaction is demonstrated in Table 3 where Fock elements of orbitals across the atoms are listed at large separations. These elements, which are shown to not vanish at "infinite" separations, are responsible for the spurious energy gain. The corresponding elements for the improved basis set (Wachters) were verified to have vanished at sufficiently large separations and indeed the asymptotic energy value for this improved basis set corresponds to the atomic limit.

Conclusions

In this paper, we have presented some anomalies which may arise in SCF calculations. This provides a list of potential problems in calculations, which are often treated as "black box". We have mainly focused on providing a qualitative explanation for the occurrence of spatial SB at the HF level.

Traditionally, spatial SB is viewed as a competition between orbital size effects and molecular resonance effects. SB is the point where orbital size effects become more dominant than resonance effects. However, this is a description of the mechanism which underlies SB. The origins of this SB lie in the comparison of the symmetry preserving PES at the molecular region along the relevant coordinate to its extreme form along the same coordinate. Thus, SB is driven primarily by the asymptotics. If the symmetric PES reaches energy values which are higher than the expected energy of the system at the asymptotic region, a lower PES must exist. The PES corresponding to the US wave function is able to reach the correct asymptotic state from the description at the equilibrium region. However, spatial SB at the DFT level cannot always be directly related to the asymptotes due to apparent limitations in the functional as discussed above. Also, we have demonstrated that the order of breaking the spatial and spin symmetry can change with the system considered. Namely, the break of these symmetries are not directly related to each other, and instead they are driven by their appropriate asymptotic limits.

Another artifact, which may arise in SCF calculations, is due to use of a limited basis set and a constrained functional form. Similar to restrictions in the wave function leading to SB, so can limitations in the one particle basis cause artifactual behavior at the asymptotic region. A manifestation was provided with the ROHF symmetric curves of both F_2^+ and O_2^+, which lie energetically lower than the asymptotic products. This was also demonstrated for Cr_2 at the DFT level (with BLYP and B3LYP functionals).

Additionally, we have been concerned with another artifact which may arise due to limitations of the functional form used to define the SCF calculation. The limited form of the UHF wave function (combined with its ability to recouple the spins of electrons along the potential curve) can lead to spurious maxima/minima on the potential curves. UHF cannot describe smoothly enough the transitions between regions of different dominant spin coupling. This was most dramatically demonstrated with O_2^+ at the 6−31*G** basis set.

Acknowledgment. This work was supported by the Director, Office of Energy Research, Office of Basic Energy Sciences, Chemical Sciences Division of the U.S. Department of Energy under Contract No. DE-AC03-76SF00098.

References and Notes

(1) Löwdin, P.-O. *Rev. Mod. Phys.* **1963**, *35*, 496.
(2) Chandrasekher, C.; Griffith, K.; Gellene, G. *Int. J. Quantum Chem.* **1996**, *58*, 29.
(3) Cohen, R.; Sherrill, C. *J. Chem. Phys.* **2001**, *114*, 8257.
(4) Murphy, R.; Schaefer, H. F., III; Nobes, R.; Radom, L.; Pitzer, R. *Int. Rev. Phys. Chem*. **1986**, *5*, 229.
(5) Watts, J. D.; Bartlett, R. *J. Chem. Phys.* **1991**, *95*, 6652.
(6) Byrd, E. F. C.; Sherrill, C. D.; Head-Gordon, M. *J. Phys. Chem. A* **2001**, *105*, 9736.
(7) Jahn, H.; Teller, E. *Proc. R. Soc. London* **1937**, *A161*, 220.
(8) Davidson, E.; Borden, W. *J. Phys. Chem.* **1983**, *87*, 4783.
(9) Jackels, C.; Davidson, E. *J. Chem. Phys.* **1976**, *964*, 2908.
(10) McLean, A.; Lengsfield, B. H., III; Pacansky, J.; Ellinger, Y. *J. Chem. Phys.* **1985**, *83*, 3567.
(11) Allen, W. D.; Horner, D. A.; Dekock, R.; Remington, R.; Schaefer, H., III. *Chem. Phys.* **1989**, *133*, 11.

(12) Lindh, R.; Barnes, A. *J. Chem. Phys.* **1994**, *100*, 224.
(13) Engelbrecht, L.; Liu, B. *J. Chem. Phys.* **1983**, *78*, 3097.
(14) Ayala, P. Y.; Schelegel, H. B. *J. Chem. Phys.* **1998**, *108*, 7560.
(15) Voter, A.; Goddard, W., III. *J. Chem. Phys.* **1981**, *75*, 3638.
(16) Voter, A.; Goddard, W., III. *J. Am. Chem. Soc.* **1986**, *108*, 2830.
(17) Hiberty, P.; Humbel, S.; Archirel, P. *J. Phys. Chem.* **1994**, *98*, 11697.
(18) Holauer, E.; Nascimento, C. *J. Chem. Phys.* **1993**, *99*, 1207.
(19) Crawford, T.; Stanton, J.; Allen, W. D.; Schaefer, H., III. *J. Chem. Phys.* **1997**, *107*, 10626.
(20) Stanton, J.; Gauss, J.; Bartlett, R. *J. Chem. Phys.* **1992**, *97*, 5554.
(21) Barnes, A.; Lindh, R. *Chem. Phys. Lett.* **1994**, *223*, 207.
(22) Crawford, T.; Stanton, J. *J. Chem. Phys.* **2000**, *112*, 224.
(23) Gwaltney, S.; Head-Gordon, M. *Phys. Chem. Chem. Phys.* **2001**, *3*, 4495.
(24) Bauernschmitt, R.; Alhrich, R. *J. Chem. Phys.* **1996**, *104*, 9047.
(25) Sherrill, C. D.; Lee, M. S.; Head-Gordon, M. *Chem. Phys. Lett.* **1999**, *302*, 425.
(26) Bally, T.; Sastry, G. N. *J. Phys. Chem. A* **1997**, *101*, 7923.
(27) Braida, B.; Hiberty, P. C.; Savin, A. *J. Phys. Chem. A* **1998**, *102*, 7872.
(28) Grüning, M.; Gritsenko, V.; van Gisbergen, S. J. A.; Baerends, E. J. *J. Phys. Chem. A* **2001**, *105*, 9211.
(29) Cizek, J.; Paldus, J. *J. Chem. Phys.* **1967**, *47*, 3976.
(30) Paldus, J.; Cizek, J. *Chem. Phys. Lett.* **1969**, *3*, 1.
(31) Paldus, J.; Cizek, J. *J. Chem. Phys.* **1970**, *52*, 2919.
(32) Paldus, J.; Cizek, J. *J. Chem. Phys.* **1971**, *54*, 2293.
(33) Paldus, J.; Cizek, J. *Can. J. Chem.* **1985**, *63*, 1803.
(34) Burton, N. A.; Yamaguchi, Y.; Alberts, I. L.; Schaefer, H., III. *J. Chem. Phys.* **1991**, *96*, 7466.
(35) Rassolov, V.; Pople, J.; Ratner, M.; Windus, T. L. *J. Chem. Phys.* **1998**, *109*, 1223.
(36) Wachters, A. *J. Chem. Phys.* **1970**, *52*, 1033.
(37) Bauschlicher, C.; Partridge, H. *Chem. Phys. Lett.* **1994**, *231*, 277.
(38) Kong, J.; et al. *J. Comput. Chem.* **2000**, *21*, 1532−1548.
(39) Van Voorhis, T.; Head-Gordon, M. *Mol. Phys.* **2002**, *100*, 1713.
(40) Dunietz, B. D.; Van-Vorhis, T.; Head-Gordon, M. *J. Theor. Comput. Chem.* **2002**, *1*, 255.
(41) Crawford, T. D.; Sherrill, C. D.; Valeev, E. F.; Fermann, J. T.; Leininger, M. L.; King, R. A.; Brown, S. T.; Janssen, C. L.; Seidl, E. T.; Yamaguchi, Y.; Allen, W. D.; Xie, Y.; Vacek, G.; Hamilton, T. P.; Kellogg, C. B.; Remington, R. B.; Schaefer, H. F., III. PSI 3.0, development version, PSITECH, Inc., Watkinsville, GA 30677, 2000.
(42) Sherrill, C. D.; Krylov, A. I.; Byrd, E.; Head-Gordon, M. *J. Chem. Phys.* **1998**, *109*, 4171.
(43) Pauling, L. *J. Am. Chem. Soc.* **1931**, *53*, 3225.
(44) Harcourt, R. *J. Chem. Educ.* **1985**, *62*, 99.
(45) Perdew, J.; Parr, R.; Levy, M.; Balduz, J., Jr. *Phys. Rev. Lett.* **1982**, *49*, 1691.
(46) Chermette, H.; Ciofini, I.; Marioti, F.; Daul, C. *J. Chem. Phys.* **2000**, *114*, 1447.
(47) Scuseria, G.; Schaeffer, H., III. *Chem. Phys. Lett.* **1990**, *174*, 501.
(48) Andersson, K.; Roos, B.; Malquist, P.-A.; Widmark, P.-O. *Chem. Phys. Lett.* **1994**, *230*, 391.
(49) Roos, B.; Andersson, K. *Chem. Phys. Lett.* **1995**, *245*, 215.
(50) Goodgame, M.; Goddard, W., III. *Phys. Rev. Lett.* **1985**, *54*, 661.
(51) Dachsel, H.; Harrison, R.; Dixon, D. *J. Phys. Chem. A* **1999**, *103*, 152.
(52) Thomas, E., III; Murray, J.; C. J.; O.; Politzer, P. *J. Mol. Struct.-(THEOCHEM)* **1999**, *487*, 177.